


Article

# CFD Study of Diffuse Ceiling Ventilation through Perforated Ceiling Panels

Alessandro Nocente <sup>1,2,\*</sup>, Tufan Arslan <sup>3</sup>, Steinar Grynning <sup>1</sup> and Francesco Goia <sup>2</sup> 

<sup>1</sup> Sintef Community, 7465 Trondheim, Norway; steinar.grynning@sintef.no

<sup>2</sup> Department of Architecture and Technology, Norwegian University of Science and Technology (NTNU), 7491 Trondheim, Norway; francesco.goia@ntnu.no

<sup>3</sup> IT Department, Scientific Computing Section, Norwegian University of Science and Technology (NTNU), 7491 Trondheim, Norway; tufan.arslan@ntnu.no

\* Correspondence: alessandro.nocente@sintef.no

Received: 15 March 2020; Accepted: 10 April 2020; Published: 17 April 2020



**Abstract:** Diffuse Ceiling Ventilation (DCV) is a promising concept to address internal air quality and thermal comfort requirements in contemporary buildings. Sound-absorbing perforated ceiling panels are common in office rooms and can be used as air diffusers without modifications. The optimization of such systems is not a trivial procedure, and numerical simulation can represent an important tool to carry out this task. Today, most of the numerical studies on DCV are performed using porous medium models and focus on the general system performance rather than on the optimization of the diffuser design. In previous studies, a CFD model was used to optimize the size and distribution of the ceiling perforation. In the study presented in this paper, the results of simulations conducted on a full-scale three-dimensional domain and the performance comparison between a continuous and non-continuous perforation distribution are given. The results show that the non-continuous diffuser design does not disturb the internal comfort and does not introduce a negative effect in the system performance. The different configurations lead to a different air distribution in the room, but in both cases, the velocity magnitude is always well below values leading to draft discomfort.

**Keywords:** Diffuse Ceiling Ventilation (DCV); CFD; ceiling panels; comfort

## 1. Introduction

According to Zhan et al. [1], buildings in developed countries are responsible for 40% of the global energy use and for 33% of global greenhouse gas emissions. The highest energy consumption is ascribable to the heating, ventilation, and air conditioning (HVAC) systems [2]. The improvement of ventilation systems by the adoption of new technologies with less energy consumption was indicated by Wu et al. [3] as one of the most efficient approaches to limit energy use for building's operations. One of the novel concepts in strategies for ventilation is the Diffuse Ceiling Ventilation (DCV). In this approach, the ventilation air is supplied in a plenum constituted by the clearance between the ceiling slabs and the suspended ceiling. The fresh air is then distributed in the room through the suspended ceiling perforation, which acts as an air diffuser. In office buildings, it is common to have a suspended ceiling made of sound-absorbing perforated panels. The characteristics of these panels make them suitable to act as air diffusers without any modification. Previous research demonstrated that DCV presents several advantages compared to traditional duct based ventilation. The large area of the air diffuser, ideally the whole room ceiling, makes it possible to distribute a larger amount of ventilation air if compared to traditional mixing ventilation systems without increasing the air velocity. Furthermore, the large area of both the diffuser and the plenum introduces a lower pressure drop in the system, therefore reducing the energy necessary for ventilation air movement. Moreover, this solution

has a lower investment cost than traditional ventilation systems [4]. DCV was first presented by van Wagenberg and Smolders [5] as a solution to provide sufficient ventilation air to animals in livestock buildings. Jacobs et al. [6] applied the DCV as a retrofitting solution to improve the ventilation of classrooms and demonstrated an increase in indoor air quality and thermal comfort, as well as in the well-being and the concentration capacity of the students. However, it is only in the last few years that most of the research on DCV took place [3]. The research approach was largely based on experiments in controlled environments. Petersen et al. [7] and Fan et al. [8] evaluated the ventilation performance in a test chamber. Hviid and Svendsen [9] tested a full-scale ceiling in a climatic chamber using two different porous surfaces. The results showed an air change efficiency equal to fully mixed conditions, excluded any evidence of thermal discomfort, and demonstrated a very low pressure drop, yet still sufficient to support the internal pressure of the plenum and ensure a unidirectional air flow. The presence of a large volume in the plenum makes this solution attractive for coupling various air treatment systems with the ventilation, as for example heating and cooling. Zhang et al. [10] presented the results of an experimental campaign in a hot-box facility of a DCV coupled with a water based heating system in the ceiling slabs.

Experimental campaigns such as those presented above are expensive and time consuming; therefore, the use of computer simulations can be largely beneficial, at least for the preliminary design of the systems, and especially as far as parametric analyses are concerned. Energy simulations are sometimes used, but Computational Fluid Dynamics (CFD) simulations are required to have a clearer view of the air flow circulation and the possible impacts on the system efficiency and the thermal comfort (especially in terms of drafts). In Wu et al. [3], the reviewed works were classified according to three diffuse ceiling solutions, namely perforated plates, ceiling slots, and porous materials. While approximately one third of the papers made use of CFD techniques, none of them applied it directly to the perforated panels and rather concentrated on the application of the porous medium model [11,12]. One of the limitations commonly associated with the use of DCV is the uneven velocity profile of the air leaving the ceiling perforation. In fact, the air injection in the plenum takes place either in a single point such as a duct or, when the DCV is coupled with natural ventilation from an external wall, through a more or less large opening in the vertical boundaries of the plenum. In both cases, the air velocity in the plenum tends to decrease with the distance from the injection point. While the friction losses play a part in this, the main reason is the decrease in the mass flow since part of the air is already injected in the room. A proper design of the suspended ceiling can partially solve the latter limitation by selectively introducing a different pressure drop. The present work compares the performance of a continuous and a non-continuous (chessboard) ceiling panel distribution in a full-scale numerical model of a typical office room. As mentioned, the low pressure drop introduced by this ventilation system is one of the advantages, particularly important when the concept is used in connection with natural ventilation. A chessboard distribution may have a positive effect; in fact, the flow leaving the perforation will face a lower resistance, and the pressure drop will not increase despite the higher velocity in the perforation. Lower pressure drop guarantees a limited use of energy to set the fluid in motion.

## 2. Suspended Ceiling

Sound-absorbing perforated panels are commonly used in office rooms, and because of their design, these panels can carry out the function of an air diffuser without modification. Several types of perforated panels are available on the market, differing in the dimensions, perforation shape, size, and material. For this research, three perforated panels were designed based on actual commercial models; see Figure 1. All the panels had dimensions of  $600 \times 600$  mm and square perforation. The perforation size and rate are shown in Table 1.

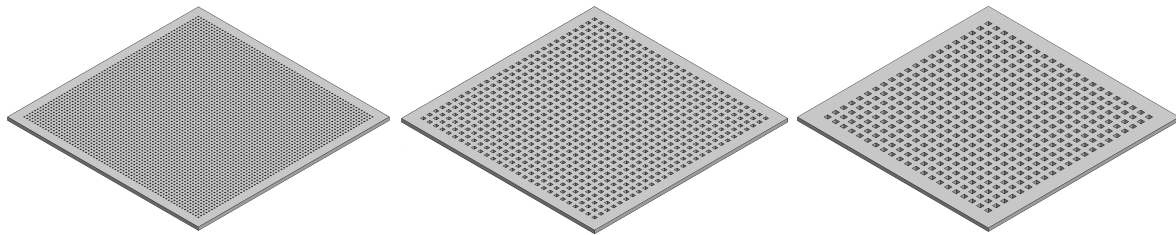


**Figure 1.** Model of the sound-absorbing perforated panels used for the numerical models [13].

**Table 1.** Perforated panels' main characteristics [13].

Panel	Perforation Size (mm)	Perforation Rate (%)
A	3 × 3	11
B	9 × 9	18
C	12 × 12	18

Each panel, when used as a ventilation diffuser, introduces a different pressure drop dependent primarily on the perforation rate, but also on the perforation size and distribution. The different pressure drop introduced is a characteristic that can be used to counteract the uneven velocity profile, previously indicated as a limitation of a system where the perforation rate is constant across the entire ceiling.

In a previous work [13], we performed a series of CFD simulations to evaluate the velocity profile of the ventilation air leaving the perforated panels for different panel configurations. The calculations were isothermal, and the only driving force for the ventilation air was assumed to be mechanical. The influence of buoyancy forces on the ventilation performance was excluded. The aim was to find an optimal distribution of the three panel perforations for a room of a certain length (namely 3.6 m). Some of the results are reported in Figure 2. The vector diagram in Figure 2a presents the results obtained using a uniform panel distribution (6 × Panel C). It is evident how the velocity profile resulted in being uneven and how the largest part of the fresh ventilation air was injected into the room in the first part of the plenum, taking the plenum inlet as the starting point. Figure 2b presents the result for one of the two optimal configurations determined in [13], a distribution of 2 Panel As, 2 Panel Bs, and 2 Panel Cs with reference to the nomenclature used in Figure 1. The order of these panel was assumed with respect to the plenum inlet taken as a starting point. In both calculations, the amount of ventilation air was kept constant and calculated according to [14]. An equally well performing configuration was found to be 3 Panel As, 2 Panel Bs, and 1 Panel C. Table 2 shows the highest and lowest velocities calculated per panel type and for each configuration in [13].

**Table 2.** Maximum and minimum velocities per panel type in the five different configurations presented in [13].

Case	Panel A		Panel B		Panel C	
	max (m/s)	min (m/s)	max (m/s)	min (m/s)	max (m/s)	min (m/s)
Case 1 (6 × A)	0.0046	0.0029				
Case 2 (6 × B)			0.005	<0.001		
Case 3 (6 × C)					0.0052	<0.001
Case 4 (3 × A + 2 × B + 1 × C)	0.0032	0.0013	0.0035	0.0018	0.002	0.0018
Case 5 (2 × A + 2 × B + 2 × C)	0.0039	0.0017	0.0044	0.0021	0.0023	0.0017

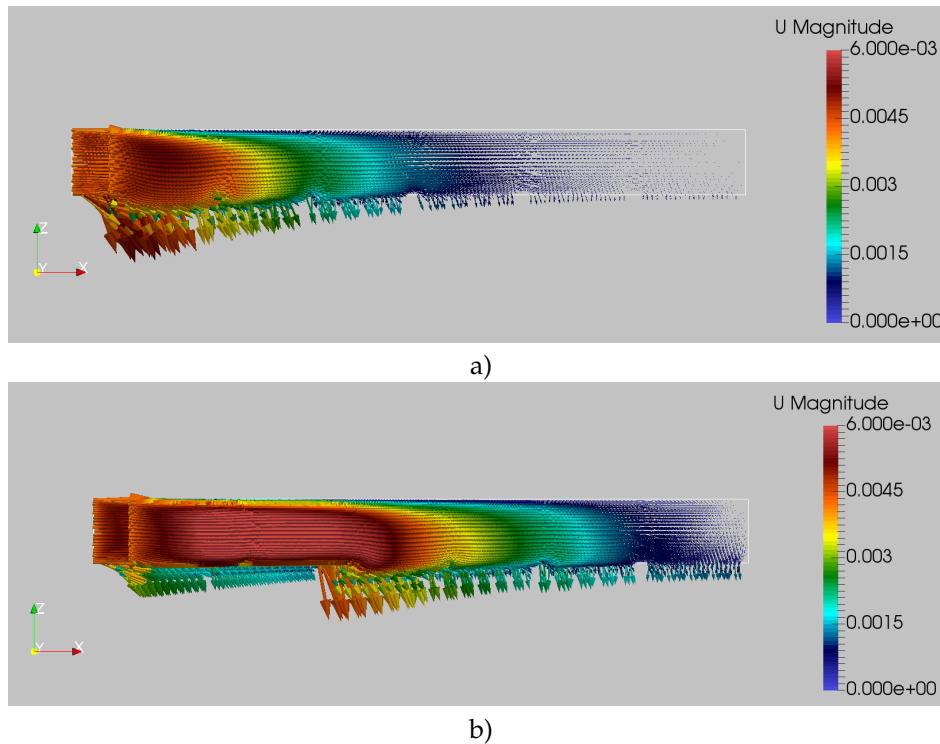


**Figure 2.** Outlet and plenum velocity distribution for different panel distributions: (a) constant panel distribution (Panel C); (b) optimized panel distribution (2× Panel A, 2× Panel B and 2× Panel C) (taken from [13]).

As Figure 2b shows, the velocity distribution is considerably more even than in Figure 2a, although a peak is still present. This situation, which could be further optimized by adapting the panel design, is however more favourable, because it presents a less pronounced peak and a shift in the peak position towards the center of the room, where occupants usually spend more time, thus improving the ventilation efficiency. The study was complemented by simulating a “room slice” to assess the influence of the panel distribution on the internal air circulation. The room slice domain consisted of a section of the room along the direction perpendicular to the plenum inlet plane, with the full room length and as wide as a panel. The suspended ceiling was therefore constituted of six panels. The results indicated that the influence of different configurations on the internal air circulation was negligible. A more comprehensive study of the “room slice” domain was carried out in [15]. Here, the isothermal hypothesis was removed to investigate the effects on the thermal comfort in the case of naturally induced airflow due to the thermal gradient between indoor and outdoor air. The outdoor temperature varied between  $-5\text{ }^{\circ}\text{C}$  and  $10\text{ }^{\circ}\text{C}$  in winter and between  $15\text{ }^{\circ}\text{C}$  and  $35\text{ }^{\circ}\text{C}$  in summer. Both winter and summer simulation had a fixed initial temperature condition, and the boundary temperatures (room walls) were kept constant ( $20\text{ }^{\circ}\text{C}$  in winter and  $26\text{ }^{\circ}\text{C}$  in summer), with the exception of the external wall, in which the boundary condition was calculated given the difference between indoor and outdoor temperature. For extreme winter and summer conditions, the authors investigated in a theoretical way the effect that a ceiling integrated conditioning system could have on the internal comfort. The solution presented a good impact on the comfort conditions in a quite large interval of outdoor temperatures. The results were promising for heating in winter, while presenting more problems such as thermal stratification in summer conditions and the necessity of further investigations.

In this work, one of the optimal configurations was tested in a full-scale room model, in two different configurations: a full ceiling panel distribution and a chessboard distribution (Figure 3). As explained, some aspects related to a chessboard configuration might have a positive impact on the ventilation efficiency while still delivering a sufficient amount of ventilation air. One of these aspects can be the lower pressure that the system needs to overcome at the ceiling perforation. Another strictly

fluid dynamics related aspects can be the positive impact of the entrainment phenomena in the volume below the ceiling. The third possible positive impact can be a saving in the panels cost together with the possibility of using the non-perforated areas for diverse installations.

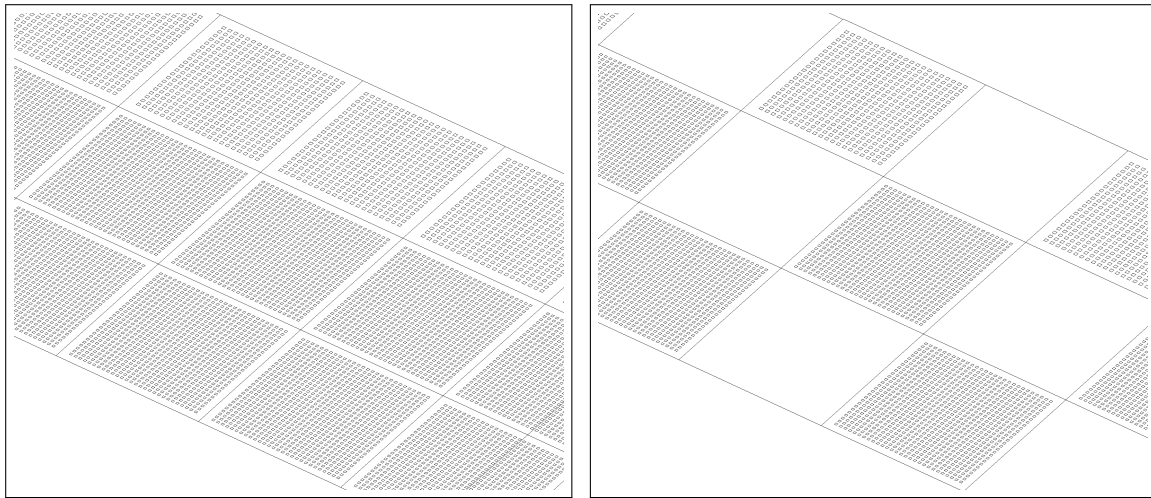


**Figure 3.** Full ceiling panel distribution (left) and chessboard panel distribution (right).

### 3. Methods

#### 3.1. Computational Domain

CFD simulations were performed on the computational domain shown in Figure 4. The volume consisted of a room with dimensions of ( $W \times L \times H$ )  $3.6 \text{ m} \times 3.6 \text{ m} \times 3 \text{ m}$ . The plenum had the same horizontal area and a height of  $0.35 \text{ m}$ . The inlet to the plenum was the area indicated in green (Figure 4) with dimensions of ( $W \times H$ )  $3.6 \text{ m} \times 0.35 \text{ m}$ . The outlet configuration was chosen taking into account the low ventilation flow rate entering the room [16]. Two different outlets were alternatively used, here referred to as Outlet 1 and Outlet 2. Outlet 1 was modeled over a square extraction duct with dimensions  $0.3 \times 0.3 \text{ m}$ , located on one of the side walls (i.e., normal to the plane containing the inlet area). Outlet 2 was located on the plane parallel to the inlet plane, ideally where the door would be located, and it was an opening at the bottom of the wall with a height of  $0.05 \text{ m}$ . These configurations were chosen to test two common solutions for ventilation air exhaust: a dedicated duct and a passage between partition walls (e.g., from the room to the corridor, then from there to the main exhaust). The suspended ceiling was constituted by the panels reported in Table 1 in a 3-2-1 configuration (see Figure 4), this being one of the optimal configurations identified in [13], and it was modeled as a two-dimensional surface. For the chessboard case, the ceiling configuration was the same, except for the replacement of every second panel (alternatively per each row) with a non-perforated surface (Figure 3).

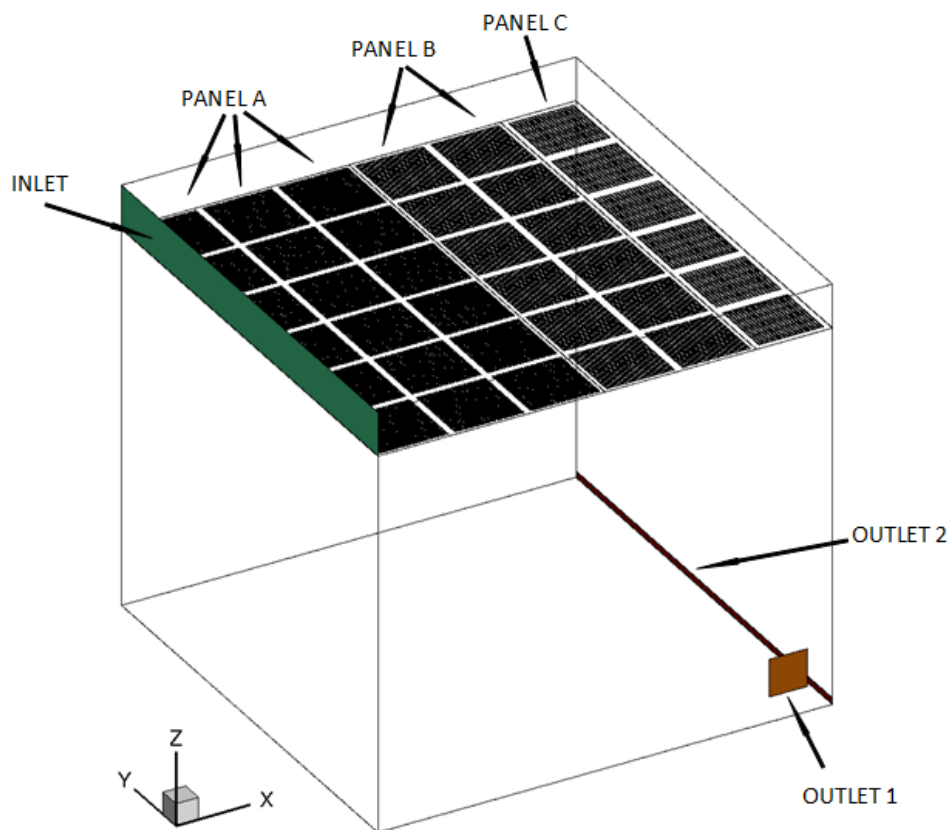


Figure 4. Computational domain.

### 3.2. Numerical Model

Due to the presence of panel perforation, the numerical simulations required a very fine mesh, capable of calculating the flow in the small holes, as well as in the main volume of the room. Figure 5 shows a close view of the ceiling mesh, where the cells colored in green represent the suspended ceiling perforation.

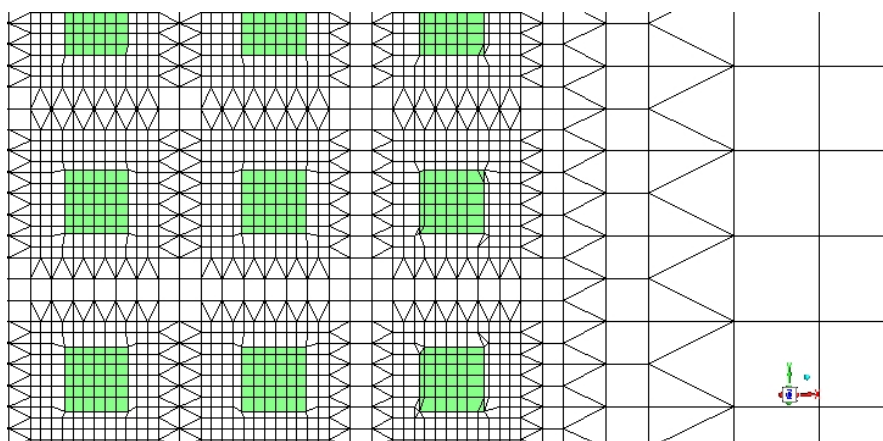
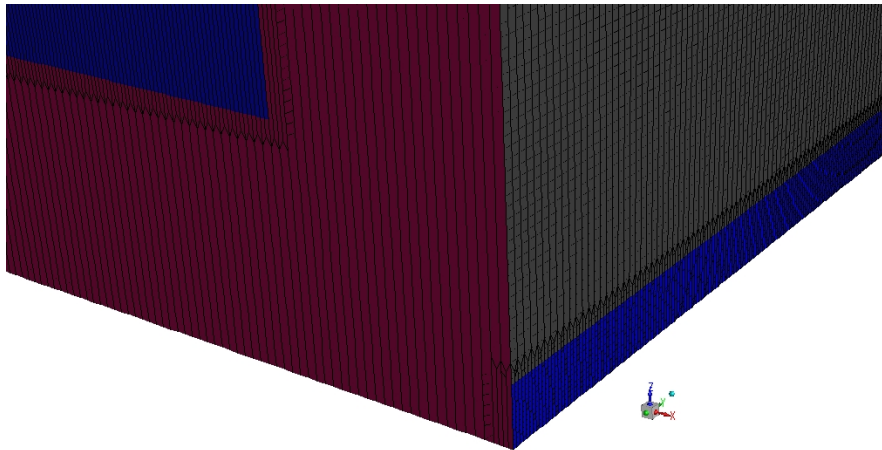


Figure 5. Particulars of the suspended ceiling mesh. In green is indicated the perforation area.

The computational domain consisted of 120 million cells, which had polyhedral and Cartesian shapes. Figure 6 is the particulars of the room volume mesh. The two areas colored in blue are the room outlets, switched in the simulations as two options.



**Figure 6.** Room volume mesh. In blue, the room outlets.

All the simulations were carried out using the software ANSYS Fluent [17]. The calculation made use of an isothermal unsteady Reynolds-averaged Navier–Stokes (URANS) model (Equations (1) and (2)), with a SIMPLE pressure-velocity coupling and a second order upwind spatial discretization. URANS is preferred to the steady-state Reynolds-averaged model (RANS) to ensure a stable numerical performance of the calculation.

$$\frac{\partial \rho}{\partial t} + \nabla(\rho U) = 0 \quad (1)$$

$$\frac{\partial U}{\partial t} + U \nabla U = -\frac{\nabla P}{\rho} + \nu \nabla^2 U + g \quad (2)$$

The turbulence was calculated with a standard k- $\epsilon$  model, Equations (3) and (4):

$$\frac{\partial(\rho k)}{\partial t} + \nabla(\rho k U) = \nabla \left( \frac{\mu_t}{\rho k} \nabla k \right) + 2\mu_t E_{ij} E_{ij} - \rho \epsilon \quad (3)$$

$$\frac{\partial(\rho \epsilon)}{\partial t} + \nabla \left( \frac{\mu_t}{\rho \epsilon} \nabla \epsilon \right) + C_{1\epsilon} \frac{\epsilon}{K} 2\mu_t E_{ij} E_{ij} - C_{2\epsilon} \frac{\epsilon^2}{K} \quad (4)$$

The k- $\epsilon$  model was chosen as it is the most widely used and validated turbulence model to simulate mean flow characteristics for the flow conditions with applications ranging from industrial to environmental flows, and it has been highly popular for inner flows. The standard variant of k- $\epsilon$  is used for simplicity and the basic requirement of initial and boundary conditions of turbulent quantities. The complexity of the model in terms of dimensions, perforation, and high density mesh requires a considerable computational effort. The simulations ran in the supercomputer Vilje [18] hosted by NTNU, using a total of 256 cores (16 nodes), and required around 300 GB RAM. The simulations were conducted in the transient state, assuming a time step  $\Delta t = 0.05$  s and 1000 steps. The calculation wall time was around 24 h. The boundary conditions imposed on the model were constant inlet velocity and a constant outlet pressure. The velocity at the inlet of the plenum was calculated to provide a ventilation air flow of  $2.4 \text{ m}^3/\text{h}$  per square meter of room floor area. The boundary condition for the outlet was set to 0 Pa gauge pressure. All the calculation were isothermal since the study focused on the fluid-mechanics problem without considering effects induced by different air density. A constant initial air density was used ( $\rho_{air} = 1.225 \text{ kg/m}^3$ ).

#### 4. Results

The results are presented as the average over all the time steps of the transient state simulations. Tables 3 and 4 display the overview of the value calculated in the domain. The first two lines show the value of the average z velocity component and the average mass flow rate in the volume directly below

the perforated ceiling. The first was calculated considering all the panels of the same type; the mass flow rate, instead, was averaged along the whole area of the ceiling section containing a certain type of panel (i.e., the same area in the continuous and the chessboard case, including the non-perforated panels in the latter). This choice was due to the different perforation rates of the panels and gave a more direct idea of how the air velocity out of the diffuser increased while keeping constant the amount of ventilation air injected.

**Table 3.** Calculated quantities in the continuous and chessboard distributions for Outlet Configuration 1.

Configuration Outlet 1 Continuous Distribution				Configuration Outlet 1 Chessboard Distribution			
Panels	A	B	C	Panels	A	B	C
Average z velocity (m/s)	0.0025	0.0064	0.0077	Average z velocity (m/s)	0.0059	0.0013	0.0014
Mass flow rate (full surface avg) (kg/s)	0.0023	0.006	0.0037	Mass flow rate (full surface avg) (kg/s)	0.0026	0.0059	0.0033
Pressure drop (Pa)	0.01			Pressure drop (Pa)	0.01		
Max velocity (m/S)	0.13 (at the outlet)			Max velocity (m/S)	0.13 (at the outlet)		

**Table 4.** Calculated quantities in the continuous and chessboard distributions for Outlet Configuration 2.

Outlet Configuration 2 Continuous Distribution				Outlet Configuration 2 Chessboard Distribution			
Panels	A	B	C	Panels	A	B	C
Average z velocity (m/s)	0.0025	0.0064	0.0077	Average z velocity (m/s)	0.0059	0.0013	0.0014
Mass flow rate (full surface avg) (kg/s)	0.0022	0.006	0.0036	Mass flow rate (full surface avg) (kg/s)	0.0026	0.0059	0.0033
Pressure drop (Pa)	0.0034			Pressure drop (Pa)	0.0034		
Max velocity (m/S)	0.063 (at the outlet)			Max velocity (m/S)	0.063 (at the outlet)		

The pressure drop was calculated as the average over all the time steps of the difference between the pressure at the plenum inlet and the pressure at the room outlet. The maximum velocity was the highest value reported (as the vector magnitude) inside the whole room, the parameter of interest to analyze the possible cause of discomfort created by drafts. In all cases, the maximum air velocity calculated in the whole volume was low and concentrated in the immediate surroundings of the outlet in configuration Outlet 1.

The average velocity fields (Vel\_mean in the contours) are shown in Figures 7–10. On the left side, the contour shows the velocity values on three horizontal planes, while on the right side, a more detailed contour of the top planes is shown, for each of the cases. The three planes were respectively the plane at 4 cm below the perforation, the horizontal mid-plane of the room volume (i.e., half of the distance between the suspended ceiling and the floor), and the plane that cut in the middle Outlet 1 surface. For the alternative configuration (Outlet 2), the bottom plane was kept at the same height. Therefore, it did not show the velocity field at the outlet, but gave a better comparative view of the room velocity field. The distance of the top plane from the perforation was chosen considering that distance to be sufficient for a full development of the flow leaving the ceiling diffuser.

Figures 11–14 show the streamline representation of the flow from the plenum inlet to the room outlet. In particular, the left part of each figure presents two planes parallel to the xz-plane, therefore roughly parallel to the main direction of the flow (from inlet to outlet). The planes were placed respectively at a distance  $y = 0.8$  m and  $y = 3$  m from the origin of the reference system (lower-right corner in Figure 11, left). The right part presented two planes parallel to the yz-plane, roughly cutting the inlet-outlet flow. In this case, the position of the planes was respectively  $x = 0.66$  m and  $x = 3.28$  m. The domains in the right part were slightly rotated to avoid the superimposition of the planes for better visualization.



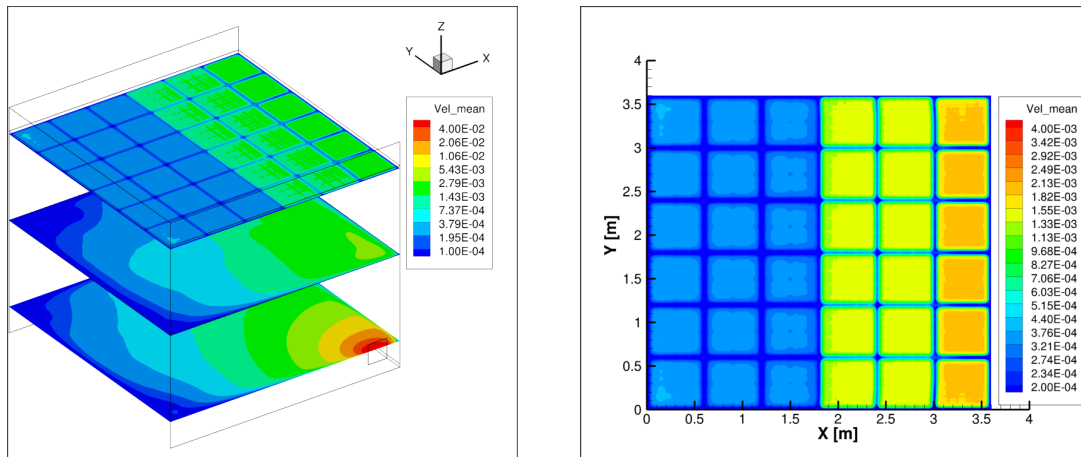


**Figure 7.** Velocity contour: three horizontal planes (left); the top plane below the ceiling (right) for the continuous distribution in configuration Outlet 1.

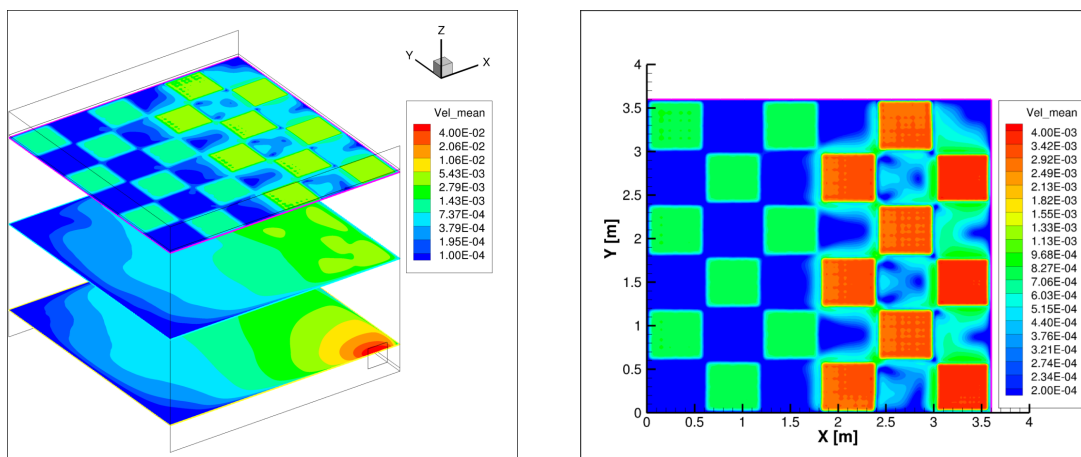


**Figure 8.** Velocity contour: three horizontal planes (left); the top plane below the ceiling (right) for the chessboard distribution in configuration Outlet 1.

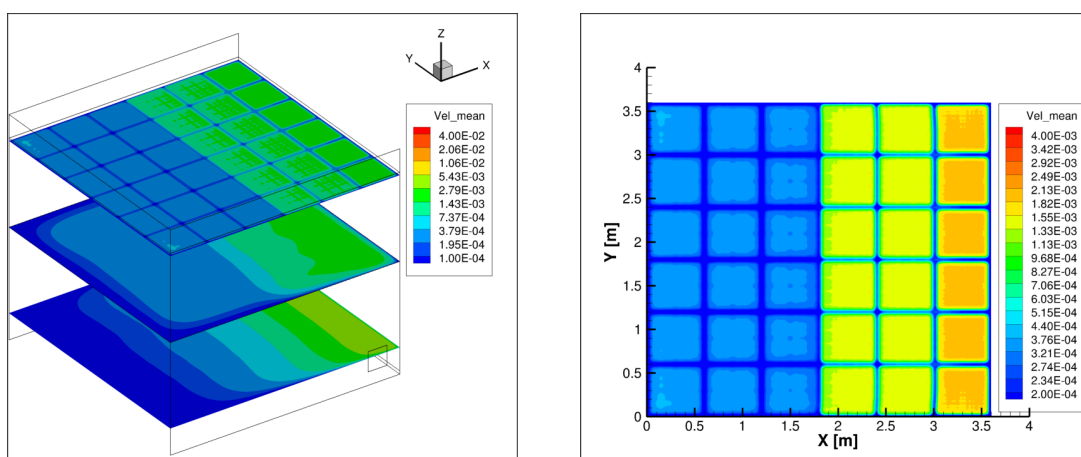


**Figure 9.** Velocity contour: three horizontal planes (left); the top plane below the ceiling (right) for the continuous distribution in configuration Outlet 2.

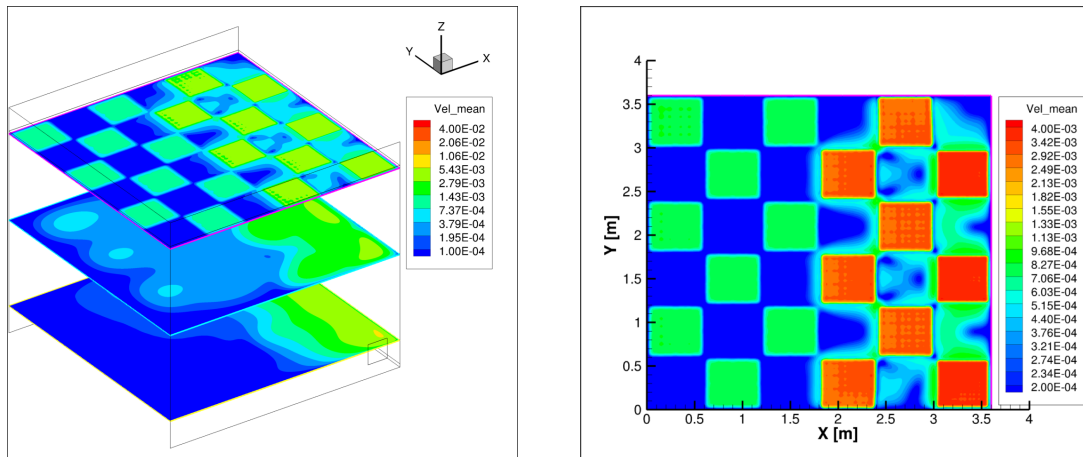


**Figure 10.** Velocity contour: three horizontal planes (left); the top plane below the ceiling (right) for the chessboard distribution in configuration Outlet 2.

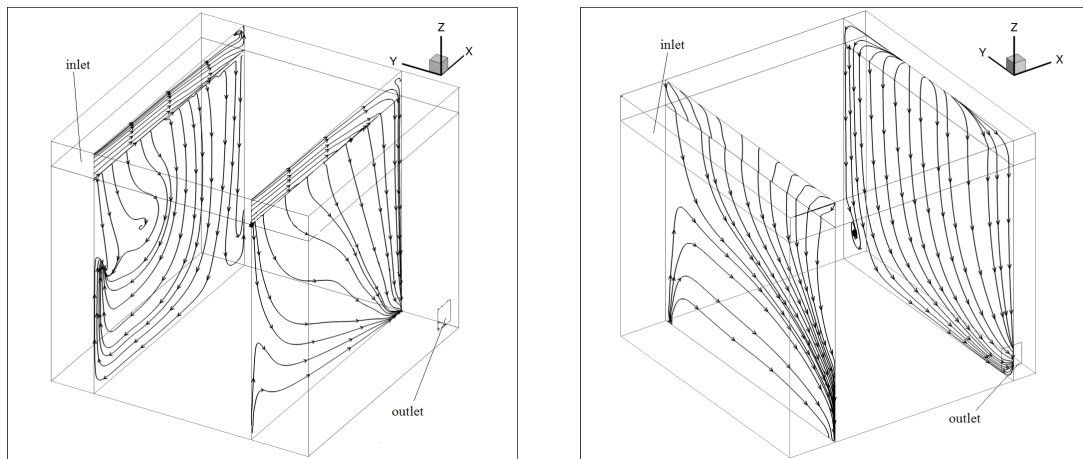


**Figure 11.** Streamlines for the continuous distribution and Outlet 1 configuration.

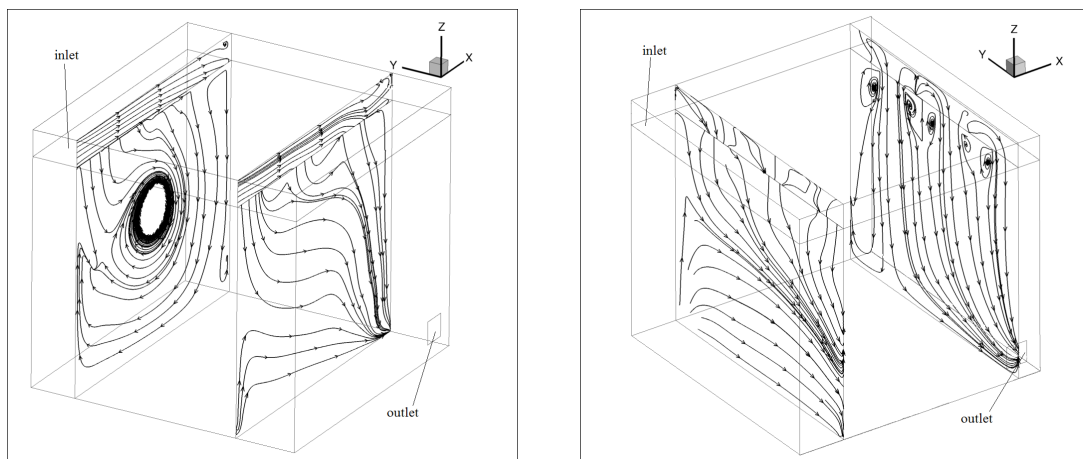


**Figure 12.** Streamlines for the chessboard distribution and the Outlet 1 configuration.

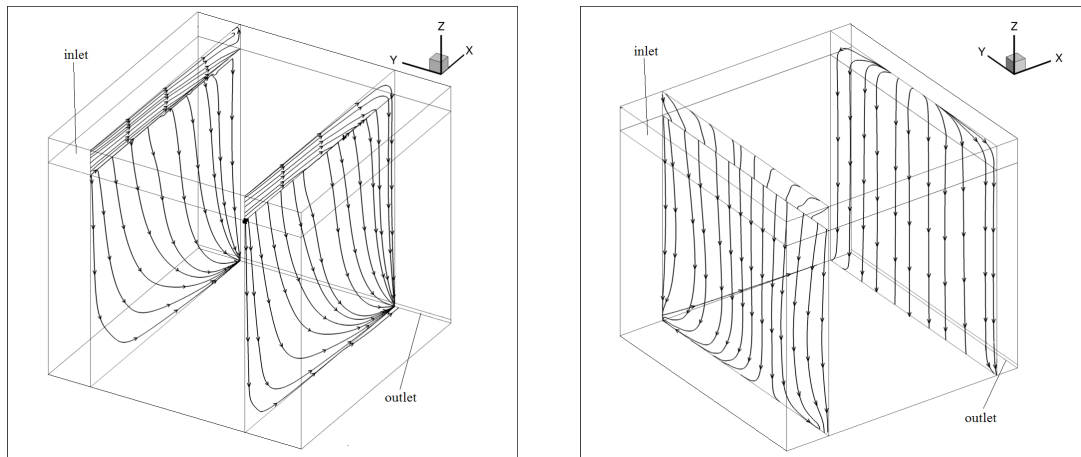


**Figure 13.** Streamlines for the continuous distribution and the Outlet 2 configuration.

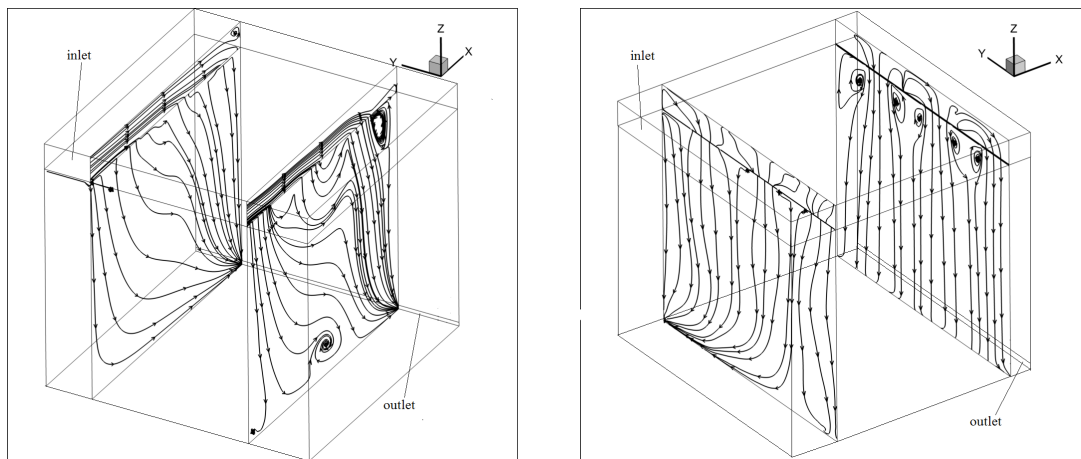


**Figure 14.** Streamlines for the chessboard distribution and the Outlet 2 configuration.

## 5. Discussion

The results in Tables 3 and 4 show that the average velocity (along the z-axis) reached a higher value when the chessboard configuration was adopted in both configurations. This was expected due to the reduced diffuser outlet area and the constant flow rate at the plenum inlet. The ventilation air flow average on the area containing the same panels, both in the continuous and chessboard distribution, remained in fact comparable. All the configurations introduced a very small pressure drop in the system. It is interesting to underline that a difference in the pressure drop could be seen for configurations with different outlets, while no significant difference appeared evident between the two ceiling configurations. This evidence suggested that the choice of the room outlet influenced to a higher extent the pressure drop of the system if compared to the choice of ceiling configuration. The maximum air velocity in the whole room volume was below the discomfort limit in the configuration Outlet 2. In the configuration Outlet 1, the maximum velocity magnitude could exceed 0.1 m/s, but this happened in a small fraction of the volume [19] surrounding the outlet.

The ceiling contours (right) in Figures 7–10 showed a velocity distribution at the ceiling outlet in line with [13], with small differences. A general increase in the velocity magnitude was seen in the chessboard configuration, as expected. Nevertheless, each configuration did not show a substantial difference with the two different outlets. This suggested that the choice of the outlet did not influence the performance of the DCV. The latter seemed, instead, more influenced by the choice of the outlet geometry. The mid-plane of Figures 9 and 10, both in the configuration Outlet 2, presented in fact a generally lower velocity. In particular, in Figure 10, it is possible to identify three zones with higher

velocity on the mid-plane otherwise not visible in Figure 8. This meant that the jet flow originating from the first row of the panels reached the midsection of the room without too much disturbance. However, the low velocity region of these sections did not represent a problem for the internal comfort.

The influence of the outlet configuration could be seen in the streamline representation as well (Figures 11–14). The flow patterns with the same outlet were comparable. In general, the Outlet 2 configuration, as expected because of the geometrical features, translated into a more even flow pattern with streamlines mostly perpendicular to the ceiling plane. The Outlet 1 configuration, instead, seemed to produce a vortex around an axis parallel to the ceiling plane and perpendicular to the outlet plane. The flow pattern may have an effect on the air quality in the room, but the characterization or quantification of this was not the object of the present study. As far as internal comfort conditions were concerned, due to the very low velocity, no relevant negative influence was expected. Independently of the outlet configuration, the chessboard panel distribution (Figures 12 and 14) showed vortex structures in the volume immediately below the perforation. This was evident especially in the plane furthest from the plenum inlet. In this zone, entrainment phenomena were likely to take place. The influence of the entrainment in the system efficiency and comfort parameter was not part of this study, but it is nevertheless one of the most interesting aspects to investigate in the future.

## 6. Conclusions

The results of the full-scale simulations presented in this paper contribute to characterizing the impact that the DCV has on the internal comfort conditions of a typical office room. It delivered a sufficient amount of ventilation air ensuring the absence of draft and working with a low pressure drop along the whole system.

The comparison between the full ceiling and the chessboard distribution showed that, although the total diffuser area was halved, thus doubling the velocity of the air leaving the diffuser, this did not translate into a significant increase in the air velocity inside the room. In both cases, the air velocity was below the discomfort limit. The velocity magnitude reached higher values in the surrounding of the outlet. The chessboard panel distribution, despite increasing the air velocity, did not show any influence on the dynamic performance of the ventilation system in terms of pressure drop. The present calculations suggested a beneficial effect of the chessboard distribution. A more marked influence of the outlet choice was instead observed.

The phenomenon behind this beneficial influence could be related to a positive entrainment effect favored by the air jets leaving the ceiling diffuser. In any case, further investigation is necessary to evaluate and give an estimate of this effect. The simulation presented in this work was isothermal and focused on the system performance rather than on the possible onset of air draft that might impact the thermal comfort. In the further development of this work, the isothermal hypothesis will be removed to investigate mainly two aspects of the problem: first, the influence of the occupants and how the thermal buoyancy caused by people, computers, and other sources of internal gain will influence the ventilation efficiency causing pressure losses and consequent back flow in the plenum; second, the investigation will involve a study of the thermal comfort in the room when natural ventilation is used with air injection directly from outdoors.

The use of CFD simulation to evaluate the efficiency and the performance of DCV is a very valuable tool in the design of these systems. Despite the large computational effort associated with the use of the presented model, the numerical investigation still represents an economical alternative to the experimental verifications on a physically built system. Furthermore, it can reveal the occurrence of phenomena that, at first sight, might not be trivial. CFD, in fact, gives all detailed visualization of the three-dimensional flow field in the room, which is hard to produce in the experiments. However, CFD has its own challenges. It always has numerical errors depending on the spatial resolution of the computational grid and assumption in the numerical models. In the present work, the focus was on the efficiency of a DCV system and the impact of different configurations on the efficiency of the ventilation system, and therefore, the CFD model used was isothermal. Nevertheless, several phenomena such as

the outdoor climate, the presence of occupants, and their behavior have a role in the air distribution efficiency. Although some of these aspects can be included in a CFD code, the complexity of the problem can become excessive, making the experimental validation fundamental for the final assessment of the solution. The evaluation of an eventual change in the sound-absorbing properties of this kind of panels when used as air diffusers was not the object of this paper. A series of experimental measurements on this will be a valuable research result. An experimental campaign involving tracer gas and pressure difference measurements on DCV is planned at the moment. The results will contribute to the validation and the eventual tuning of the computational model.

**Author Contributions:** Conceptualization, A.N., F.G., and S.G.; methodology, A.N., T.A., and F.G.; software, T.A.; formal analysis, A.N. and T.A.; data curation, T.A. and A.N.; writing, original draft preparation, A.N.; writing, review and editing, A.N., T.A., and F.G.; visualization, T.A.; supervision, F.G. and S.G.; project administration, S.G.; funding acquisition, S.G. and F.G. All authors read and agreed to the published version of the manuscript.

**Funding:** This work was supported by the Research Council of Norway and several partners through the project “Advanced facades with integrated technology – SkinTech” (No. 255252).

**Acknowledgments:** The authors wish to thank Uninett/Sigma for the support and the computing time.

**Conflicts of Interest:** The authors declare no conflict of interest.

## References

1. Zhan, J.; Liu, W.; Wu, F.; Li, Z.; Wang, C. Life cycle energy consumption and greenhouse gas emissions of urban residential buildings in Guangzhou city. *J. Clean. Prod.* **2018**, *194*, 318–326. [[CrossRef](#)]
2. Sun, X.; Gou, Z.; Lau, S.S.Y. Cost-effectiveness of active and passive design strategies for existing building retrofits in tropical climate: Case study of a zero energy building. *J. Clean. Prod.* **2018**, *183*, 35–45. [[CrossRef](#)]
3. Wu, W.; Yoon, N.; Tong, Z.; Chen, Y.; Lv, Y.; Aerenlund, T.; Benner, J. Diffuse ceiling ventilation for buildings: a review of fundamental theories and research methodologies. *J. Clean. Prod.* **2019**, *211*, 1600–1619. [[CrossRef](#)]
4. Zhang, C.; Yu, T.; Heiselberg, P.K.; Pomianowski, M.Z.; Nielsen, P.V. *Diffuse Ceiling Ventilation-Design Guide*; Department of Civil Engineering, Aalborg University: Aalborg, Denmark, 2016.
5. Van Wagenberg, A.V.; Smolders, M. Contaminant and heat removal effectiveness of three ventilation systems in nursery rooms for pigs. *Trans. ASAE* **2002**, *45*, 1985. [[CrossRef](#)]
6. Jacobs, P.; van Oeffelen, E.C.; Knoll, B. Diffuse ceiling ventilation, a new concept for healthy and productive classrooms. In Proceedings of the Indoor Air 2008, Copenhagen, Denmark, 17–22 August 2008; Volume 3.
7. Petersen, S.; Christensen, N.; Heinsen, C.; Hansen, A. Investigation of the displacement effect of a diffuse ceiling ventilation system. *Energy Build.* **2014**, *85*, 265–274. [[CrossRef](#)]
8. Fan, J.; Hviid, C.; Yang, H. Performance analysis of a new design of office diffuse ceiling ventilation system. *Energy Build.* **2013**, *59*, 73–81. [[CrossRef](#)]
9. Hviid, C.A.; Svendsen, S. Experimental study of perforated suspended ceilings as diffuse ventilation air inlets. *Energy Build.* **2013**, *56*, 160–168. [[CrossRef](#)]
10. Zhang, C.; Heiselberg, P.K.; Pomianowski, M.; Yu, T.; Jensen, R.L. Experimental study of diffuse ceiling ventilation coupled with a thermally activated building construction in an office room. *Energy Build.* **2015**, *105*, 60–70. [[CrossRef](#)]
11. Mikeska, T.; Fan, J. Full scale measurements and CFD simulations of diffuse ceiling inlet for ventilation and cooling of densely occupied rooms. *Energy Build.* **2015**, *107*, 59–67. [[CrossRef](#)]
12. Zhang, C.; Heiselberg, P.; Chen, Q.; Pomianowski, M. Numerical analysis of diffuse ceiling ventilation and its integration with a radiant ceiling system. *Build. Simul.* **2017**, *10*, 203–218. [[CrossRef](#)]
13. Nocente, A.; Grynning, S.; Mathisen, H.M.; Goia, F. Computational fluid dynamics study of a diffuse ceiling ventilation system through perforated sound absorbing ceiling panels. In Proceedings of the Roomvent & Ventilation 2018, Espoo, Finland, 2–5 June 2018; pp. 899–904.
14. ISO 15251:2007. Indoor Environmental Input Parameters for Design and Assessment of Energy Performance of Buildings Addressing Indoor Air Quality, Thermal Environment, Lighting and Acoustics. 2007. Available online: <https://shop.bsigroup.com/ProductDetail/?pid=00000000030133865> (accessed on 17 April 2020)

15. Nocente, A.; Goia, F.; Grynning, S. Numerical investigation of a diffuse ventilation ceiling system for buildings with natural and hybrid ventilation. In Proceedings of the 7th International Building Physics Conference, Syracuse, NY, USA, 23–26 September 2018; pp. 859–864.
16. Zhang, C.; Heiselberg, P. Diffuse ceiling ventilation. *Rehva J.* **2019**, *56*, 78–82.
17. Fluent, A. *19.2 Theory Guide*; ANSYS: Canonsburg, PA, USA, 2018.
18. Vilje. Available online: <https://www.hpc.ntnu.no/display/hpc/Vilje> (accessed on 17 April 2020 ).
19. ISO 7730:2005. *Ergonomics of the Thermal Environment-Analytical Determination and Interpretation of Thermal Comfort Using Calculation of the PMV and PPD Indices and Local Thermal Comfort Criteria*; ISO: Geneva, Switzerland, 2005.



© 2020 by the authors. Licensee MDPI, Basel, Switzerland. This article is an open access article distributed under the terms and conditions of the Creative Commons Attribution (CC BY) license (<http://creativecommons.org/licenses/by/4.0/>).